A defect in a novel ADAMTS family member is the cause of the belted white-spotting mutation

Cherie Rao[1,*], Dorothee Foernzler[1,*], Stacie K. Loftus[2], Shanming Liu[1], John D. McPherson[3], Katherine A. Jungers[4], Suneel S. Apte[4], William J. Pavan[2] and David R. Beier[1,*,†]

[1]Genetics Division, Brigham and Women's Hospital, Harvard Medical School, Boston, MA 02476, USArr
[2]National Human Genome Research Institute, National Institutes of Health, Bethesda, MD 02115, USA
[3]Department of Genetics, Washington University, St. Louis, MO 20892, USA
[4]Department of Biomedical Engineering, Cleveland Clinic Foundation, Cleveland, OH 44195, USA
*These authors contributed equally to this work
[†]Author for correspondence (e-mail: beier@rascal.med.harvard.edu)

Accepted 22 May 2003

Development 130, 4665-4672

doi:10.1242/dev.00668

Summary

Several features of the pigment defect in belted (*bt*) mutant mice suggest that it occurs as a result of a defect in melanocyte development that is unique from those described for other classical white-spotting mutations. We report here that *bt* mice carry mutations in *Adamts20*, a novel member of the ADAMTS family of secreted metalloproteases. *Adamts20* shows a highly dynamic pattern of expression in the developing embryo that generally precedes the appearance of melanoblasts in the same region, and is not expressed in the migrating cells themselves. *Adamts20* shows remarkable homology with *GON-1*, an ADAMTS family protease required for distal tip cell migration in *C. elegans*. Our results suggest that the role of ADAMTS proteases in the regulation of cell migration has been conserved in mammalian development.

Key words: ADAMTS, White-spotting, Melanocyte migration, Mouse

Introduction

Mutations affecting coat color and pattern are among the earliest and most well studied genetic variants in the mouse. The first demonstration of linkage in a mammalian system was carried out in 1915 by Haldane and colleagues using the coat color mutations albino (*c*) and pink-eye dilution (*p*) (Haldane et al., 1915). As of 1945, the murine genetic map contained 26 loci in 10 linkage groups; 11 of these were mutations affecting pigmentation (Dickie, 1954). The characterization of these loci by positional cloning has provided considerable insight into fundamental developmental processes. For example, the characterization of the agouti (*a*) locus has illuminated complex patterns of melanocyte regulation (reviewed by Voisey and van Daal, 2002). Studies of the various coat color dilution loci, including dilute (*d*), ashen (*ash*) and leaden (*ln*), have revealed the molecular mechanisms that are required for intracellular transport (Matesic et al., 2001; Mercer et al., 1991; Wilson et al., 2000).

The white-spotting mutations, which affect the maturation and survival of neural crest-derived melanoblasts, have been particularly enlightening regarding the developmental mechanisms required for normal lineage determination, migration and proliferation. Notable among these was the determination that the tyrosine kinase receptor *Kit* is mutated in dominant spotting (*W*) and its ligand stem cell factor (*Scf*; *Kitl* – Mouse Genome Informatics) is the gene mutated in steel mice (*Sl*). Studies of the lethal spotting (*ls*) and piebald (*s*) mouse mutants, which are characterized by mutations in endothelin 3 (*Edn3*) and its G-protein coupled receptor endothelin-B receptor (*Ednrb*), respectively, illustrate the obligatory requirement for endothelin-signaling in pigment cell development similar to that of *Scf/Kit* (Baynash et al., 1994; Hosoda et al., 1994). Abnormalities in the transcription factor *Mitf* results in the microopthalmia (*mi*) mutation (Hodgkinson et al., 1993) and a defect in the sry-related homeobox gene *Sox10* results in dominant megacolon (*Dom*) (Southard-Smith et al., 1998). Recent studies have shown how these signaling pathways intersect (Potterf et al., 2000; Wu et al., 2000).

The belted (*bt*) locus is one of the few 'classic' white-spotting mutations yet to be characterized. It presents as a mostly pigmented mouse except for a region proximal to the hindlimbs that appears as a white belt. The first allele of this mutation was identified in 1945 (Murray and Snell, 1945) and many additional alleles have been identified. Skin-neural tube recombination experiments provided conflicting results regarding the embryonic cell type that is defective during development (Mayer and Maltby, 1964; Schaible, 1972). These studies were re-interpreted by Silvers in light of Mintz's hypothesis about the clonal development of melanoblast precursors; Silvers concluded that *bt* mice have a number of unviable melanoblast clones, most of which are replaced by melanoblasts migrating from neighboring viable clones. However, the belt region remains non-pigmented because it is growing too rapidly to be repopulated (Silvers, 1979).

We report that *bt* is due to a defect in a novel ADAMTS (a disintegrin-like and metalloprotease (reprolysin type) with thrombospondin type I motif) protein, which is a member of a large family of secreted metelloproteases that are presumed to

interact with the extracellular matrix (ECM). The gene encoding a homologous and highly similar protease, *GON-1*, has been shown to play a crucial role in cell migration in *C. elegans*. Our results suggest this function has been conserved in mammalian development. Notably, our analysis demonstrates that the *bt* gene product is not made by melanocytes themselves, but rather by the mesenchyme through which these cells migrate. This result implies that there is a highly coordinated and dynamic pattern of gene expression in the developing embryo that is required for the proper localization of neural-crest-derived cells.

Materials and methods

Crosses

Congenic C57BL/6J (B6) bt^{Bei1}/+ mice are maintained in our mouse facility. The original *bt* mutation is carried in the ABP strain, which was obtained from The Jackson Laboratory. B6.I-4 bt^{Mri1} were generously provided by George Carlson (McClaughlin Insitute). DBA/2J (D2) and *Mus castaneus* (CAST) mice were obtained from The Jackson Laboratory. For recombination analysis, F1 B6/D2 bt^{Bei1}/+ mice or F1 B6/CAST bt^{Bei1}/+ mice were intercrossed and affected progeny identified by examination. Microsatellite markers polymorphic between strains were chosen using information provided by the Genome Center at the Whitehead Institute (http://www-genome.wi.mit.edu/cgi-bin/mouse/index#genetic). PCR primers were purchased from Research Genetics, Genomic DNA preparation and PCR analysis was carried out according to standard techniques.

Physical mapping

Screening of two YAC libraries identified one clone of 300 kb that contained the flanking microsatellite markers. Using these markers as anchors, a contig of BAC clones was established by BAC walking. Three contig BAC clones were obtained by screening a 129/Sv BAC library (Genome Systems, St Louis, MO) with PCR-amplified STSs from adjacent BAC clone ends. All STS fragments were mapped using either mouse radiation hybrids or a C57BL/6J × *M. spretus* backcross to ensure their appropriate map location. The contig was confirmed by direct sequencing of BAC clones using STS-specific primers. *Hin*dIII digests of the three BAC clones revealed a similar restriction pattern suggesting a substantial overlap between them. The BAC-end sequences were used to generate oligonucleotide probes, and filters containing spotted clones from the RPCI-23 B6 library was hybridized using the 'overgo' strategy (Ross et al., 1999). Twelve clones were identified and STS-content mapped and three clones were sequenced (RP23-24F24, Accession Number AC084384; RP23-5K17, Accession Number, AC084382; RP23-54K18, Accession Number AC084385) (Fig. 1).

Molecular cloning

Shotgun sequencing of BAC clones in the *bt* region identified several fragments with homologies to ADAMTS family proteases. Primers corresponding to an internal part of the presumptive transcript were designed from these regions (Adex 3/8F, 5′-GGCTTAG-CAGAGCTAGGCACCC-3′; and Adex3/8R, 5′-GTTGTCACC-ACCACACAC-3′) and an RT-PCR product (Adex3/8) was generated from embryonic and skin mRNA. A transcript carrying the full-length open reading frame was identified using 5′ and 3′ RACE analysis from commercially prepared mouse embryonic day 15 Marathon RACE-ready cDNA according to the manufacturer's instructions (Clontech) A longer transcript containing additional TSP domains was obtained by generating primers corresponding to the presumptive transcript identified on the basis of comparative genomic analysis. The shorter transcript can be uniquely identified using a primer pair in which the reverse primer is derived from a region of its 3′ terminus that is not contained in the larger transcript: BtXF (5′-TAATGCCAGTA-CCAAGCCCGAGTC-3′) and Adamts3′R1 (5′-GTAAAAGGAA-CGTGGTCATAAGCC-3′) (1143 bp product). The longer transcript can be uniquely identified using the primer pair: TS20mid3′F (5′-GTAGCATGCAGGACTGAGAAC-3′) and 2R long end (5′-TGGTCTGAAACCCCAATGAGCAC-3′) (835 bp). Three different *bt* mutant alleles were characterized by sequencing overlapping cDNA fragments derived from embryonic mRNA using primers distributed across the transcript. Sequence changes were confirmed by analysis of genomic DNA.

Expression analysis

Northern analysis was done using the Origene Multi-tissue PolyA+ Northern blot (Origene) and the Mouse Embryo MTN blot (Clontech). Hybridization was carried out with the probes Adex 3/8 and TS20mid3′F/2R (described above) using standard techniques. For in situ analysis, FVB/NJ mouse embryos were fixed overnight in 4% paraformaldehyde in PBS. Date of plug formation was noted as E 0.5. Reverse transcribed digoxigenin-conjugated probes were made from linearized plasmids, DCT cDNA (Steel et al., 1992) and Adex3/8. Whole-mount in situ hybridizations were performed using published protocols (Wilkinson and Nieto, 1993) with modifications as detailed elsewhere (Loftus et al., 2002). In situ hybridization analysis on tissue sections were done using standard techniques as previously described (Somerville et al., 2003).

Results

We identified a mouse with a recessive mutation causing a belted phenotype in our analysis of a congenic C57BL/6J (B6) strain of mouse carrying the perinatal lethality (*ple*) transgene insertion (Beier et al., 1989). The appearance of the belt was similar to that of the original *bt* mutation and the mutation was determined to be an allele of *bt* because it failed to complement when crossed with a known *bt* mutant mouse (Fig. 1). It appeared not to be due to an insertion event, as it was found to segregate from the *ple* transgene (data not shown).

The assignment of *bt* to distal mouse chromosome 15 was already known from previous mapping studies (Silvers, 1979). To determine the precise location by high-resolution-mapping, homozygous *bt* mice were crossed with wild-type DBA/2J and *M. castaneus* (CAST) mice and their F1 *bt*/+ progeny were intercrossed or backcrossed. The homozygous *bt* offspring were analyzed using microsatellite markers from distal mouse chromosome 15. As CAST mice are more distantly related to B6 than are DBA/2J, the frequency of polymorphism in the B6×CAST cross was higher, which has allowed us to define at high resolution the *bt*-containing interval. Several unresolved microsatellite markers closely linked to *bt* were ordered by using DNA from a reference cross between B6 and *M. spretus*, the EUCIB backcross panel (European Backcross Collaborative Group, 1994).

In the analysis of over 1500 meioses, we identified five recombinants between *D15Mit108* and *D15Mit272*, the microsatellite markers most closely flanking the *bt* locus. No recombinants were found between *bt* and *D15Mit 245*. Using these markers as anchors, a contig of BAC clones derived from a 129/Sv genomic library covering the interval was established as described in the Materials and methods. Single-strand conformational polymorphism (SSCP) analysis of the recombinants using primers derived from BAC end-sequence narrowed the interval carrying the mutation further (Fig. 2).

To use the publicly funded B6 mouse sequencing effort, it

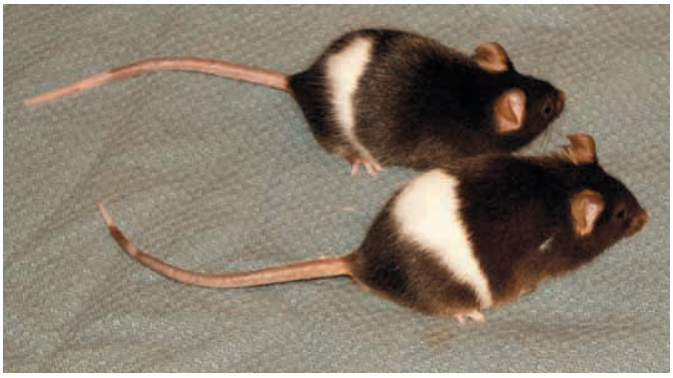

Fig. 1. Identification of a novel *bt* allele. The lower mouse is homozygous for bt^{Bei1}. The upper mouse is derived from a cross between a homozygous bt^{Bei1} mouse and a mouse homozygous for the original *bt* allele, demonstrating that the two mutations fail to complement and are therefore allelic.

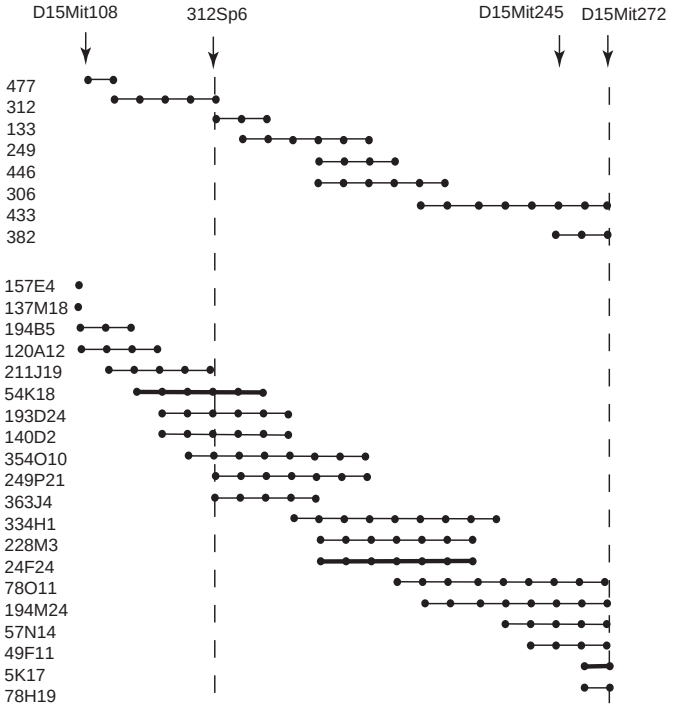

Fig. 2. Physical map of the *bt* locus. The top panel includes BAC clones obtained from a 129/Sv-genomic library. The bottom panel includes BAC clones obtained from a C57BL/6-genomic library. Black circles correspond to STSs obtained from BAC ends and used to order clones in the contig. Broken lines show the recombinant interval defined by the flanking markers 312Sp6 (an SSCP found using BAC end sequences) and D15Mit272 (an SSLP). The three BAC clones that were sequenced are shown with thick horizontal lines (RP23-24F24, Accession Number AC084384; RP23-5K17, Accession Number AC084382; RP23-54K18, Accession Number AC084385).

was necessary to generate a B6 BAC contig covering the *bt* recombinant interval. The BAC-end sequences we had obtained from our analysis of the 129/Sv-derived clones were used to generate oligonucleotide probes, and filters containing spotted clones from the RPCI-23 B6 library were hybridized with the pooled probes. Twelve clones were identified and STS-content mapped and three clones were sequenced (Fig. 2).

BLAST analysis of the genomic sequence identified a region with homology to the ADAMTS family of metalloproteases. No other homologies to sequences in the non-redundant or EST databases were identified. Primers corresponding to an internal part of the presumptive transcript were designed and an RT-PCR product was generated from mouse embryonic and skin mRNA. Northern analysis using this probe identified a transcript in embryonic polyA-containing mRNA (see below). A 4644 bp full-length transcript was identified using 5′ and 3′ RACE. This contained a 1425 amino acid open reading frame, most closely related to the human ADAMTS9 gene (Fig. 3). In consultation with the Mouse and Human Gene Nomenclature Committees (www.informatics.jax.org/mgihome/nomen/ and www.gene.ucl.ac.uk/nomenclature/), this novel family member has been designated *Adamts20*.

To assess whether *Adamts20* is the gene affected in the *bt* mutation, we analyzed three different *bt* alleles: our spontaneous mutation (bt^{Bei1}), the original *bt* mutation (carried in the ABP strain), and a spontaneous *bt* mutation identified by George Carlson and colleagues (bt^{Mri1}). RT-PCR products were generated from embryonic mRNA obtained from homozygous mutant mice. All three contain mutations affecting the protein sequence. The original *bt* allele carries a C to T mutation at position 1598 that results in the substitution of leucine for proline in the ADAM cysteine-rich domain. The bt^{Mri1}allele carries an A to C mutation at position 4073 that results in the substitution of proline for histidine. The bt^{Bei1} allele carries a C to T mutation at position 2860 that generates a stop codon, resulting in a truncation of the protein that removes 471 C-terminal amino acids (Fig. 3). These sequence changes are not present in DNA from the parental background of these mutant mice (DBA/2, B6.I-4 and B6, respectively).

Northern analysis of poly-A-containing mRNA from adult tissue showed barely detectable expression in skin only (data not shown). Analysis of embryonic mRNA identified a major transcript of 8 kb that increased in abundance from day E11 to E17 (Fig. 4), as well as two additional bands at E17. In situ hybridization analysis of whole-mount embryos revealed a highly dynamic pattern of expression (Fig. 5). Specifically, *Adamts20* expression in the neural tube is visible at E9.5-11.5. This precedes expression of the melanoblast marker DCT, which is expressed in the developing pigmented retinal epithelium of the eye at E9.5 and in migrating melanoblasts at E10.5. By E11.5 *Adamts20* expression has extended laterally from the neural tube along the sides of the embryo with increased density surrounding the base of the limb buds. Again, this expression of *Adamts20* precedes expression of DCT detected in migrating melanoblasts in the same region, which are visible at E12.5 but not at E11.5.

In situ hybridization also reveals that *Adamts20* expression is found in a variety of embryonic tissues (data not shown). Initially, *Adamts20* is detectable in the dorsal neural tube and a line of cells immediately lateral to the neural tube, as well as around the base of the limb buds. Craniofacial expression is present in the first pharangeal arch and also at the cleft between the medial nasal processes. By E12.5, expression appears in the developing vibrissae follicle and the boundary between the developing nasal process and the telencephalon. Expression is

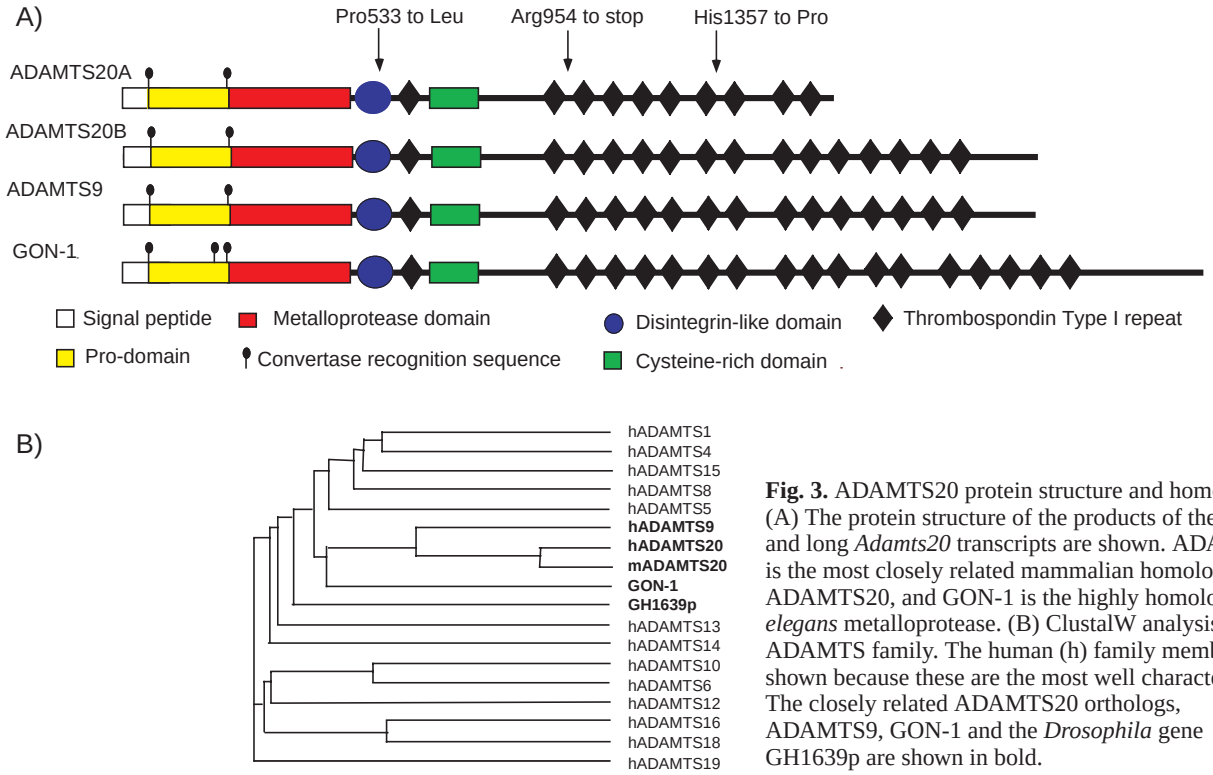

Fig. 3. ADAMTS20 protein structure and homologies. (A) The protein structure of the products of the short and long *Adamts20* transcripts are shown. ADAMTS9 is the most closely related mammalian homolog of ADAMTS20, and GON-1 is the highly homologous *C. elegans* metalloprotease. (B) ClustalW analysis of the ADAMTS family. The human (h) family members are shown because these are the most well characterized. The closely related ADAMTS20 orthologs, ADAMTS9, GON-1 and the *Drosophila* gene GH1639p are shown in bold.

also first visible in the condensing mammary gland and within the developing digits. By E14.5 *Adamts20* expression is found in the vibrissae follicles of the snout and in the hair follicles of the skin. Expression of Adamts20 was examined in more detail in the developing skin using in situ hybridization on sections of E13.5-18.5. Skin expression was mainly in the dermis at E13.5 (Fig. 6A,B) and more highly expressed in the vibrissae follicles of the snout and hair follicles of the skin at later ages (Fig. 6C-H).

The human ortholog of *Adamts20* has been characterized, and resides in the expected region of conserved synteny on human chromosome 12q12 (Somerville et al., 2003). The transcript for this gene is larger than that identified for the mouse, and has a longer open reading frame that contains an additional four TS repeats. Examination of the genomic region distal to mouse *Adamts20* indicated that exons encoding corresponding sequences were present. Primers were designed corresponding to a presumptive larger transcript, and RT-PCR products containing these regions contiguous with the previously described open reading frame were identified. Several lines of evidence suggest that the shorter cDNA product represents a bona fide alternative transcript of *Adamts20*. First, the shorter transcript was identified using 3′ RACE and contains a poly-A sequence. The genomic sequence does not contain a poly-A stretch at the same region, indicating this product is not an artifact of mis-priming by oligo dT at an internal site on a larger transcript. In addition, hybridization of a probe containing sequence unique to the larger transcript does not identify the major band in embryonic mRNA (Fig. 4). Rather, two fewer abundant transcripts are found at a later time-point. Quantitation of the mRNA products using a dilution method provides supporting evidence that the shorter transcript is more abundant in the embryo (data not shown).

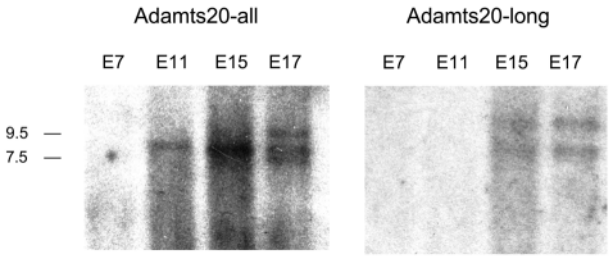

Fig. 4. *Adamts20* expression during embryogenesis. *Adamts20* expression was assayed by northern hybridization of polyA+ RNA at E7, E11, E15 and E17. The left panel (Adamts20-all) was analyzed using the Adex3/8 probe (see Materials and methods) that identifies both the short and long *Adamts20* transcripts. The right panel (Adamts20-long) was analyzed with the TS20mid3′F/2R fragment, which identifies only the long transcript.

Discussion

We have identified a novel ADAMTS family member as the gene mutated in *bt* mutant mice. Three alleles of *bt* have non-conservative sequence changes in the coding region of this gene, which is designated *Adamts20*; one of these introduces a nonsense codon that would result in a truncation of 471 C-terminal amino acids, including eight TS domains. Examination of the recent assembly of the mouse genome supports *Adamts20* as the gene affected in *bt*. In the 400 kb region covering the two BACs that contain the *bt* recombinant interval, *Adamts20* is identified as a presumptive novel gene in the Ensembl assembly. No other known or predicted genes are identified in this region. Notably, the distal recombinant SSLP marker *D15Mit272* resides only 5 kb away from *Adamts20*, and

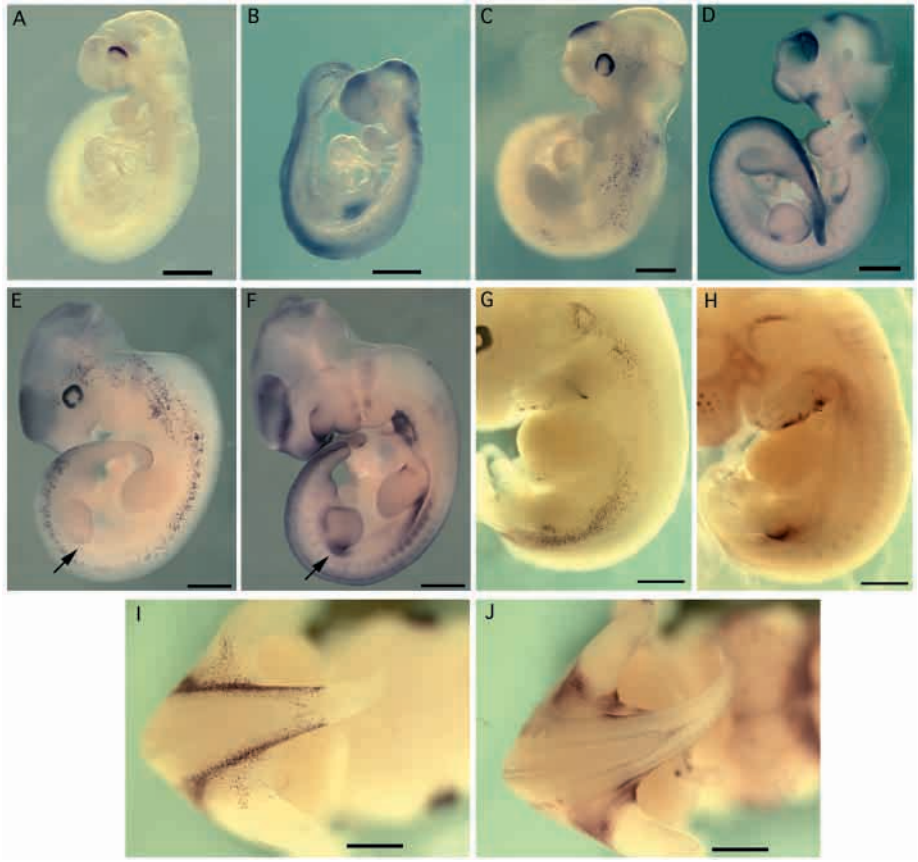

Fig. 5. *Adamts20* expression is distinct and precedes that of melanoblast marker DCT. *Adamts20* expression (B,D,F,H,J) is compared with that of melanoblast marker DCT (A,C,E,G,I) through developmental stages E9.5 (A,B), E10.5 (C,D), E11.5 (E,F), and E12.5 (G-J). *Adamts20* expression in the neural tube is visible at E9.5 (B), E10.5 (D) and E11.5 (F). At E9.5, DCT is expressed only the developing pigmented retinal epithelium of the eye (A) and in migrating melanoblasts at E10.5 (C). By E11.5, *Adamts20* expression has extended laterally from the neural tube along the sides of the embryo with increased density surrounding the base of the limb buds E11.5 (F) and remains expressed here through to E12.5 (H,J). This expression of *Adamts20* at the base of the limb buds (black arrows in E,F) at E11.5 precedes expression of DCT detected in migrating melanoblasts in the same region, visible at E12.5 (G,I), but not at E11.5 (E). Scale bars: 1 mm in A-D; 2 mm in E-J.

the non-recombinant SSLP marker *D15Mit245* is located within the gene.

Analysis of *Adamts20* using the simple modular architecture research tool (http://smart.embl-heidelberg.de/) reveals that it has the protein motifs found in other family members, including a propeptide typical in length of the ADAMTS family, a reprolysin-type catalytic domain, a disintegrin-like domain, an ADAMTS cystein-rich domain, a spacer devoid of cysteines and a TS repeat (TSR1) (Hurskainen et al., 1999). The C-terminal region of ADAMTS-20A, the short product of *Adamts20*, contains an additional eight TS domains; the long product ADAMTS-20B, which is generated by an alternatively spliced mRNA, carries six more TS domains (for a total of 14). While this paper was in review, the independent identification of mouse *Adamts20* was reported (Llamazares et al., 2003). This corresponds to the long product we have identified. Expression of this gene in adult tissue was analyzed using northern and western analysis, and found primarily in brain and testes. Metalloprotease activity was demonstrated using a peptide substrate.

The ADAMTS protease family comprises 19 distinct gene products that are also present in invertebrates. Like most secreted metalloproteases, the ADAMTS enzymes are secreted as pro-enzymes, which are activated in the secretory pathway

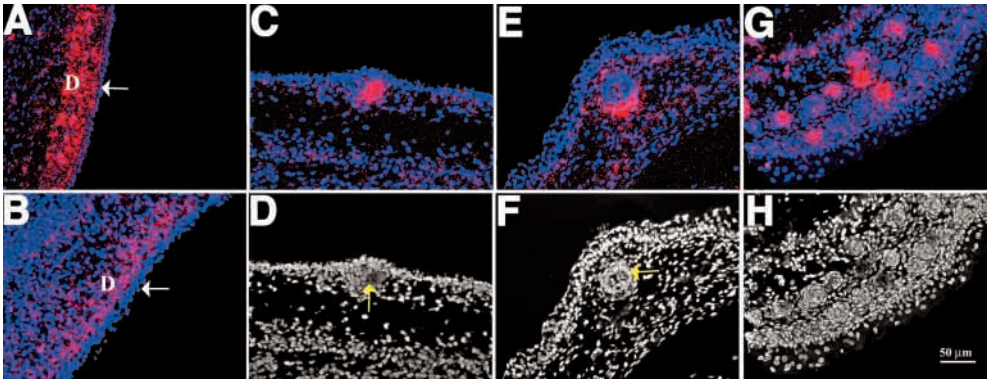

Fig. 6. *Adamts20* is expressed in the dermis. Radioactive in situ hybridization of *Adamts20* expression during mouse skin development at E13.5 (A), E14.5 (B), E15.5 (C,D), E17.5 (E,F) and E18.5 (G,H). In A and B, the arrows indicate the epidermis where no hybridization is seen and D indicates labeling of cells in the dermis. In C,E,G, labeling of dermis is seen, as well as intense hybridization of cells in epidermal appendages. The arrows in corresponding DAPI-stained images illustrate hair follicles in D,F. (G,H) Images from the snout region showing intense staining in vibrissae follicle. Images A-C,E,G use red pseudocolor to identify silver grains viewed under dark-field illumination and blue staining corresponds to DAPI-stained nuclei viewed under UV light. Images D,F,H show DAPI staining alone of the same images shown in C,E,G, respectively. Scale bar: 50 μm.

or at the cell surface by pro-protein convertases such as furin. Important functions in development and in human disease have been ascertained for some of these enzymes. ADAMTS1, ADAMTS4 and ADAMTS5 are believed to mediate loss of cartilage aggrecan in arthritis (Tortorella et al., 1999). *ADAMTS13* mutations cause inherited thrombocytopenic purpura (Levy et al., 2001), and autoantibodies to this enzyme may be the cause of acquired forms of the disease. Mutations in *ADAMTS2* in humans cause a severe inherited skin fragility (Ehlers-Danlos syndrome type VIIC or dermatosparactic type) that was first detected in a variety of animal species and termed dermatosparaxis (Colige et al., 1999; Nusgens et al., 1992).

As is the case for all white-spotting mutants, the melanocyte deficiency found in *bt* mice may be the result of any of a number of mechanisms, including the disruption of neural crest formation, specification of the melanoblast lineage, proliferation, survival, migration throughout the embryo, migration from dermis to epidermis, entry into the hair follicle or differentiation into any of the various stages of melanocyte development. *Adamts20*^{bt}/*Adamts20*^{bt} mice are unique among the classic spotting mutants in several ways. First, the mouse mutants that have early effects on melanocyte development such as *Ednrb*^{s}/*Ednrb*^{s} and *Edn3*^{ls}/*Edn3*^{ls} demonstrate more extensive ventral spotting than dorsal spotting (Dunn and Charles, 1937). This is thought to be due to an early reduction in melanoblast numbers that fail to proliferate and migrate sufficiently to populate the entire embryos, thus leaving the furthest migratory portions devoid of melanoblasts (Pavan and Tilghman, 1994). However, *Adamts20*^{bt}/*Adamts20*^{bt} mice demonstrate a more pronounced dorsal than the ventral spotting, suggesting that this mutation acts later in development. Furthermore, in addition to exhibiting regional defects in hair pigmentation, *Kit*^{W}/+, *Scf*^{Sl}/+, *Ednrb*^{s}/*Ednrb*^{s}, *Ednrb*^{s}/+, *Edn3*^{ls}/*Edn3*^{ls} and *Edn3*^{ls}/+ mice have a reduction of melanocytes in hardarian gland, membraneous labyrinth, choroids, leg musculature and ankle skin, indicating a widespread defect in melanocyte function. However *Adamts20*^{bt}/*Adamts20*^{bt} mice have a melanocyte reduction restricted only in the hair follicles in the white belt region, suggesting a more restricted mode of action. Taken together with the presumptive role of *Adamts20* as a metalloprotease, these findings suggest that *Adamts20*^{bt} disrupts a melanocyte developmental pathway that is unique from those described for other spotting mutations.

Mayer and Maltby (Mayer and Maltby, 1964) have examined the etiology of white-spotting in *Adamts20*^{bt} mice using embryonic grafting experiments. Areas of skin from presumptive white spotted and pigmented areas of E12-12.5 *Adamts20*^{bt}/*Adamts20*^{bt} embryos were grafted into coelom of the chick and allowed to form skin and hair. Grafts obtained from presumptive pigmented areas developed pigmented hairs and melanocytes in the dermis of the graft and in the coelom of the host. However, most grafts from white spotted regions displayed unpigmented hairs, yet had extensive melanocytes in the dermis between the follicles and in the coelom, suggesting neural crest-derived melanocytes could function normally in supportive environments. Mayer and Maltby concluded that the melanoblasts were able to occupy the entire skin graft from the white spotted area but were unable to form differentiated melanocytes within the hair follicles in this region. They propose that *Adamts20*^{bt} mutation acts at the hair follicle to either not allow entry of melanoblasts or to not support their differentiation into functioning melanocytes within the follicular environment. Our observation that *Adamts20* is expressed in the developing dermis at E13.5 and in hair follicles at later embryonic ages is consistent with this conclusion. However, as previously noted, other investigators obtained conflicting results in similar experiments (Schaible, 1972), and Silvers has suggested that the results obtained in both studies could be due to effects on the progenitor melanoblast population (Silvers, 1979).

The potential role of *Adamts20* may perhaps be best inferred from the analysis of distal tip cell (DTC) migration in *C. elegans* (reviewed by Lehmann, 2001). During larval development, the gonad acquires two U-shaped arms by directed migration of DTCs along the body wall basement membranes. The specific path of migration is controlled positively and negatively by several guidance factors, including netrins and TGFβ homologs. However, no DTC migration occurs in the absence of the *gon-1* gene product, which has been shown to be a ADAMTS family member with remarkable homology to *Adamts20* (37% amino acid identity and 50% similarity; Fig. 3). (Blelloch and Kimble, 1999). ClustalW analysis reveals that *Adamts20* and the highly similar *Adamts9* proteins are more closely related to the *GON-1* product than they are to other members of the ADAMTS family, which is remarkable given their evolutionary distance (Fig. 3). Genomic sequence analysis predicts the existence of a highly related *Drosophila* protein GH1639p, although nothing has yet been reported regarding its expression or function. The possible role of *Adamts20* in the regulation of migration is consistent with the observation that its closest mammalian homolog, ADAMTS-9, is located at the cell surface and can process versican, a large aggregating proteoglycan that has been implicated in neural crest cell migration (Somerville et al., 2003). One notable distinction between the proposed conservation of the role of these ADAMTS family proteases in the regulation of cell migration is that *GON-1* is expressed by the migrating DTCs, while *Adamts20* is not expressed in migrating melanocytes. However, *GON-1* is also expressed in muscle and has a role in determining gonad shape, demonstrating that this protease does have a non-cell autonomous function in *C. elegans* (Blelloch et al., 1999; Blelloch and Kimble, 1999).

Secreted metalloproteinases could be required for cell migration by virtue of a relatively nonspecific modification of the ECM such that it is permissive for cell transit. Alternatively, metalloproteinases may be required for specific processing of secreted guidance factors. This is of particular significance, given the well-characterized roles of secreted factors such as *Scf* and *Edn3* in melanoblast migration. Of note is the fact that two mutant *Kit* alleles, *W*^{sash} and *W*^{banded}, have a belt when heterozygous. Both of these mutations show ectopic expression of *Kit* during embryogenesis due to genomic rearrangements (Duttlinger et al., 1993; Kluppel et al., 1997). It has been suggested that this ectopic expression might sequester soluble SCF, reducing the amount of ligand available to migrating melanoblasts and reducing their survival by a non-cell autonomous mechanism. The possible role of secreted metalloproteases in developmental regulation is supported by evidence that the induction of matrix metalloproteinase 9 (MMP9) in bone marrow cells results in the release of soluble

SCF (Heissig et al., 2002). The authors conclude that this enables bone marrow repopulating cells to translocate to a permissive vascular niche, favoring differentiation and reconstitution of the stem/progenitor cell pool.

In situ analysis of *Adamts20* expression during embryogenesis reveals a remarkably dynamic pattern of expression. Given this dramatically changing pattern, one might expect that a mutation in *Adamts20* would have a more severe embryonic phenotype. The mild phenotype found in *bt* mutant mice may be due to functional redundancy within the ADAMTS metalloprotease family. However, it is notable that all of the mutations found in the *bt* mice are well downstream of the metalloprotease domain. These secreted mutant proteins may therefore retain partial activity, and the *bt* mutation may thus represent a hypomorphic rather than a null phenotype. A counterpoint to this argument is the evidence from other ADAMTS mutations that suggests these alleles could also result in a near complete loss of function. Naturally occurring mutations in ADAMTS2 and ADAMTS13 cause amino acid changes in the ancillary domains of the respective proteases, yet there is near complete or complete loss of function (Levy et al., 2001). Additionally, analysis of the processing of aggrecan by ADAMTS4 and versican by ADAMTS9 provides biochemical evidence that the protease domains do not function in the absence of the ancillary domains (Tortorella et al., 2000; Somerville et al., 2003). Ultimately, an engineered null mutation of *Adamts20* will be necessary to address these possibilities.

Finally, the rapidly changing pattern of *Adamts20* expression during development implies a tightly regulated signaling interaction between the tissues that express this protease and the population of cells whose migration it influences. It will be of considerable interest to identify the substrates for this enzyme whose proteolysis presumably underlies the belted phenotypes, as well as the transcriptional mechanisms that facilitate the coordinated expression during melanoblast migration of *Adamts20* and other signaling molecules such as *Kit* and *Scf*.

This work was supported by NIH grants HD29028 (to D.R.B.) and AR049930 (to S.S.A.) and HG02155 (to J.D.M.). We also thank Dr Lynne Lamoreux for helpful discussions.

References

Baynash, A. G., Hosoda, K., Giaid, A., Richardson, J. A., Emoto, N., Hammer, R. E. and Yanagisawa, M. (1994). Interaction of endothelin-3 with endothelin-B receptor is essential for development of epidermal melanocytes and enteric neurons. *Cell* **79**, 1277-1285.

Beier, D. R., Morton, C. C., Leder, A., Wallace, R. and Leder, P. (1989). Perinatal lethality (ple): A mutation caused by integration of a transgene into distal mouse chromosome 15. *Genomics* **4**, 498-504.

Blelloch, R., Anna-Arriola, S. S., Gao, D., Li, Y., Hodgkin, J. and Kimble, J. (1999). The gon-1 gene is required for gonadal morphogenesis in Caenorhabditis elegans. *Dev. Biol.* **216**, 382-393.

Blelloch, R. and Kimble, J. (1999). Control of organ shape by a secreted metalloprotease in the nematode Caenorhabditis elegans. *Nature* **399**, 586-590.

Colige, A., Sieron, A. L., Li, S. W., Schwarze, U., Petty, E., Wertelecki, W., Wilcox, W., Krakow, D., Cohn, D. H., Reardon, W. et al. (1999). Human Ehlers-Danlos syndrome type VII C and bovine dermatosparaxis are caused by mutations in the procollagen I N-proteinase gene. *Am. J. Hum. Genet.* **65**, 308-317.

Dickie, M. M. (1954). Expanding knowledge of the genome of the mouse. *J. Natl. Cancer Inst.* **15**, 679.

Dunn, L. C. and Charles, D. (1937). Studies on spotting patterns. *Genetics* **22**, 14-42.

Duttlinger, R., Manova, K., Chu, T. Y., Gyssler, C., Zelenetz, A. D., Bachvarova, R. F. and Besmer, P. (1993). W-sash affects positive and negative elements controlling c-kit expression: ectopic c-kit expression at sites of kit-ligand expression affects melanogenesis. *Development* **118**, 705-717.

European Backcross Collaborative Group (1994). Towards high resolution maps of the mouse and human genomes – a facility for ordering markers to 0.1 cM resolution. *Hum. Mol. Genet.* **3**, 621-627.

Haldane, J. B. S., Sprunt, A. D. and Haldane, N. M. (1915). Reduplication in mice. *J. Genet.* **5**, 133-135.

Heissig, B., Hattori, K., Dias, S., Friedrich, M., Ferris, B., Hackett, N. R., Crystal, R. G., Besmer, P., Lyden, D., Moore, M. A. et al. (2002). Recruitment of stem and progenitor cells from the bone marrow niche requires MMP-9 mediated release of kit-ligand. *Cell* **109**, 625-637.

Hodgkinson, C. A., Moore, K. J., Nakayama, A., Steingrimsson, E., Copeland, N. G., Jenkins, N. A. and Arnheiter, H. (1993). Mutations at the mouse microphthalmia locus are associated with defects in a gene encoding a novel basic-helix-loop-helix-zipper protein. *Cell* **74**, 395-404.

Hosoda, K., Hammer, R. E., Richardson, J. A., Baynash, A. G., Cheung, J. C., Giaid, A. and Yanagisawa, M. (1994). Targeted and natural (piebald-lethal) mutations of endothelin-B receptor gene produce megacolon associated with spotted coat color in mice. *Cell* **79**, 1267-1276.

Hurskainen, T. L., Hirohata, S., Seldin, M. F. and Apte, S. S. (1999). ADAM-TS5, ADAM-TS6, and ADAM-TS7, novel members of a new family of zinc metalloproteases. General features and genomic distribution of the ADAM-TS family. *J. Biol. Chem.* **274**, 25555-25563.

Kluppel, M., Nagle, D. L., Bucan, M. and Bernstein, A. (1997). Long-range genomic rearrangements upstream of Kit dysregulate the developmental pattern of Kit expression in W57 and Wbanded mice and interfere with distinct steps in melanocyte development. *Development* **124**, 65-77.

Lehmann, R. (2001). Cell migration in invertebrates: clues from border and distal tip cells. *Curr. Opin. Genet. Dev.* **11**, 457-463.

Levy, G. G., Nichols, W. C., Lian, E. C., Foroud, T., McClintick, J. N., McGee, B. M., Yang, A. Y., Siemieniak, D. R., Stark, K. R., Gruppo, R. et al. (2001). Mutations in a member of the ADAMTS gene family cause thrombotic thrombocytopenic purpura. *Nature* **413**, 488-494.

Llamazares, M., Cal, S., Quesada, V. and Lopez-Otin, C. (2003). Identification and characterization of ADAMTS-20 defines a novel subfamily of metalloproteinases-disintegrins with multiple thrombospondin-1 repeats and a unique GON-domain. *J. Biol. Chem.* **31**, 31.

Loftus, S. K., Larson, D. M., Baxter, L. L., Antonellis, A., Chen, Y., Wu, X., Jiang, Y., Bittner, M., Hammer, J. A., 3rd and Pavan, W. J. (2002). Mutation of melanosome protein RAB38 in chocolate mice. *Proc. Natl. Acad. Sci. USA* **99**, 4471-4476.

Matesic, L. E., Yip, R., Reuss, A. E., Swing, D. A., O'Sullivan, T. N., Fletcher, C. F., Copeland, N. G. and Jenkins, N. A. (2001). Mutations in Mlph, encoding a member of the Rab effector family, cause the melanosome transport defects observed in leaden mice. *Proc. Natl. Acad. Sci. USA* **98**, 10238-10243.

Mayer, T. and Maltby, E. (1964). An experimental investigation of pattern development in lethal spotting and belted mouse embryos. *Dev. Biol.* **9**, 269-286.

Mercer, J. A., Seperack, P. K., Strobel, M. C., Copeland, N. G. and Jenkins, N. A. (1991). Novel myosin heavy chain encoded by murine dilute coat colour locus. *Nature* **349**, 709-713.

Murray, J. and Snell, G. (1945). Belted, a new sixth chromosome mutation in the mouse. *J. Hered.* **36**, 266-268.

Nusgens, B. V., Verellen-Dumoulin, C., Hermanns-Le, T., de Paepe, A., Nuytinck, L., Pierard, G. E. and Lapiere, C. M. (1992). Evidence for a relationship between Ehlers-Danlos type VII C in humans and bovine dermatosparaxis. *Nat. Genet.* **1**, 214-217.

Pavan, W. J. and Tilghman, S. M. (1994). Piebald lethal (sl) acts early to disrupt the development of neural crest-derived melanocytes. *Proc. Natl. Acad. Sci. USA* **91**, 7159-7163.

Potterf, S. B., Furumura, M., Dunn, K. J., Arnheiter, H. and Pavan, W. J. (2000). Transcription factor hierarchy in Waardenburg syndrome: regulation of MITF expression by SOX10 and PAX3. *Hum. Genet.* **107**, 1-6.

Ross, M., LaBrie, S., McPherson, J. and Stanton, V. (1999). Screening large-insert libraries by hybridization. In *Current Protocols in Human Genetics* (ed. N. C. Dracopoli, J. L. Haines, B. R. Korf, D. T. Moir, C. C. Morton, C. E. Seidman, J. G. Seidman and D. R. Smith), pp. 5.6.1-5.6.52. New York, NY: John Wiley and Sons.

Schaible, R. (1972). Comparative effects of piebald-spotting genes on clones of melanocytes in different vertebrate species. In *Pigmentation: Its Genesis*

and Biologic Control (ed. V. Riley), pp. 343-357. New York: Appleton-Century-Crofts.

Silvers, W. K. (1979). *The Coat Colors of Mice*. New York: Sringer-Verlag.

Somerville, R. P., Longpre, J. M., Jungers, K. A., Engle, J. M., Ross, M., Evanko, S., Wight, T. N., Leduc, R. and Apte, S. S. (2003). Characterization of ADAMTS-9 and ADAMTS-20 as a distinct ADAMTS subfamily related to Caenorhabditis elegans GON-1. *J. Biol. Chem.* **278**, 9503-9513.

Southard-Smith, E. M., Kos, L. and Pavan, W. J. (1998). Sox10 mutation disrupts neural crest development in Dom Hirschsprung mouse model. *Nat. Genet.* **18**, 60-64.

Steel, K. P., Davidson, D. R. and Jackson, I. J. (1992). TRP-2/DT, a new early melanoblast marker, shows that steel growth factor (c-kit ligand) is a survival factor. *Development* **115**, 1111-1119.

Tortorella, M., Pratta, M., Liu, R. Q., Abbaszade, I., Ross, H., Burn, T. and Arner, E. (2000). The thrombospondin motif of aggrecanase-1 (ADAMTS-4) is critical for aggrecan substrate recognition and cleavage. *J. Biol. Chem.* **275**, 25791-25797.

Tortorella, M. D., Burn, T. C., Pratta, M. A., Abbaszade, I., Hollis, J. M., Liu, R., Rosenfeld, S. A., Copeland, R. A., Decicco, C. P., Wynn, R. et al. (1999). Purification and cloning of aggrecanase-1: a member of the ADAMTS family of proteins. *Science* **284**, 1664-1666.

Voisey, J. and van Daal, A. (2002). Agouti: from mouse to man, from skin to fat. *Pigment Cell Res.* **15**, 10-18.

Wilkinson, D. G. and Nieto, M. A. (1993). Guide to techniques in mouse development. In *Methods in Enzymology* (ed. P. M. Wassarman and M. L. DePamphilis), pp. 361-373. San Diego: Academic Press.

Wilson, S. M., Yip, R., Swing, D. A., O'Sullivan, T. N., Zhang, Y., Novak, E. K., Swank, R. T., Russell, L. B., Copeland, N. G. and Jenkins, N. A. (2000). A mutation in Rab27a causes the vesicle transport defects observed in ashen mice. *Proc. Natl. Acad. Sci. USA* **97**, 7933-7938.

Wu, M., Hemesath, T. J., Takemoto, C. M., Horstmann, M. A., Wells, A. G., Price, E. R., Fisher, D. Z. and Fisher, D. E. (2000). c-Kit triggers dual phosphorylations, which couple activation and degradation of the essential melanocyte factor Mi. *Genes Dev.* **14**, 301-312.